Distribution unlimited

Lasers For Remote Sensing At NASA

September 2005

Norman P. Barnes

NASA Langley Research Center
Hampton, VA 23681 U.S.A.

ABSTRACT

NASA is developing active remote sensors to monitor the health of Planet Earth and for exploration of other planets. Development and deployment of these remote sensors can have a huge economic impact. Lasers for these active remote sensors span the spectral range from the ultraviolet to the mid infrared spectral regions. Development activities range from quantum mechanical modeling and prediction of new laser materials to the design, development, and demonstration of instruments that can be deployed in the field.

1.0 Introduction

NASA uses remote sensing to monitor the health of Planet Earth and for exploring other worlds. Measuring the atmospheric variables is needed initially for understanding and eventually for predicting trends on Planet Earth. Monitoring the health of Planet Earth can have huge economic impacts. Remote sensing on other worlds is necessary for exploration purposes including: precision entry, descent and landing; assessment of resources; and scientific purposes.

Remote sensors deployed in satellites can monitor the entire planet. By placing a nadir viewing remote sensor in a polar orbiting satellite, north to south coverage is obtained. As the planet rotates on its axis, east to west coverage is obtained. For many scientific applications, data should be obtained on a 250 by 250 km grid at a minimum. On Earth, there are over 8000 grids of this size. Thus, a single satellite can gather the information of 8000 ground stations. In addition, an active remote sensor in a satellite samples the rarified upper

atmosphere first. Therefore, the lower density in the upper atmosphere enjoys the higher probe energies before the probe is attenuated by the higher scattering and absorption associated with the lower atmosphere.

Measurements of the atmospheric can have huge economic impacts. Ozone in the upper atmosphere is needed to block solar ultraviolet radiation. However, ozone in the lower atmosphere contributes to smog. Ozone density measurements can be made utilizing a DIAL, differential absorption lidar, system that operates in the ultraviolet. A DIAL system can make vertically resolved ozone density measurements employing a time of flight technique. Accurate measurements of aerosol size and density and altimetry often use a pair of widely separated wavelengths. This is most commonly done using Nd:YAG and is second harmonic. Global water vapor density measurements, best accomplished at 0.944 μm, can greatly improve weather forecasting and predicting the strength of hurricanes. Water vapor density measurements are also highly useful for planetary exploration, in particular on Mars. Global wind measurements are needed for better weather prediction as well as for aircraft safety and efficiency. Any wavelength longer than about 1.4 μm is sufficiently eye safe to be employed but Ho lasers operating around 2.05 μm appear to be the most suitable for coherent wind measurements from space. Measurements of carbon dioxide are needed because it is a green house gas on Earth and the primary component of the Martian atmosphere. Carbon dioxide can be measured using the same Ho laser that measures wind. Methane and carbon monoxide can be measured with a mid infrared parametric oscillator.

Lasers required for remote sensing from satellites are virtually unique devices. Although the exact specifications depend on the particular application, general specifications appear in Table I.

TABLE 1. General Laser specifications

Parameter	Specifications
Energy/pulse	1.0 J/pulse
Pulse repetition frequency	10 Hz
Pulse format	double pulses, 300 μs apart
Wavelength	match absorption, 1.0 ppm
Spectral bandwidth	1.0 pm
Environmental issues	cosmic radiation, 10g liftoff
Beam quality	TEM_{00} mode
Reliability	5 years or 5 billion shots

While some specifications, such as lifetime, are applicable to communication lasers, the totality of specifications, such as high energy as well as lifetime, make these lasers virtually unique. Specifications such as the particular wavelength and the environment are not common specifications for lasers. As a result, an extremely limited market exists for these lasers.

2.0 Ultraviolet lasers

A tunable ultraviolet laser can be constructed using a Nd:YAG laser and nonlinear optics. A straight forward method is to initially frequency double the Nd:YAG. Part of the second harmonic is used to pump a parametric oscillator or parametric oscillator and amplifier that operate around 0.715 μm. Output from the parametric oscillator and the remaining energy from the frequency doubled pulse is then used in a sum frequency process to generate an output at 0.305 μm. A $Ti:Al_2O_3$ laser could be used instead of the parametric oscillator but the timing of the second harmonic and $Ti:Al_2O_3$ pulses must be closely matched. NASA Langley has sponsored the development of the pump laser at Fibertek and the development of the parametric oscillator at Sandia.

Fibertek designed a Nd:YAG laser oscillator and amplifier system to generate the second harmonic needed for sum frequency generation and a parametric oscillator pump [1]. A side pumped slab laser configured in a seeded ring oscillator produced 50 mJ per pulse at a pulse repetition frequency of 50 Hz. A nearly stable resonator produced a beam with a beam quality M^2 of 1.5. The laser output is amplified in a pair of single side pumped, zig zag, slab amplifiers. A Dove prism reverses the beam image between the slab amplifiers. With single side pumping, the output of the second amplifier is between 0.30 and 0.35 J per pulse. The efficiency of the oscillator and amplifier is about 0.07 [1]. With double side pumped slab amplifiers, the laser output energy is projected to be greater than 1.0 J per pulse.

Sandia devised a sophisticated design for the parametric oscillator [2]. A simplified diagram is displayed in Figure 1. A nonplanar ring resonator is the heart of the system. In order to simplify the optical diagram, the optics needed for nonplanar operation are not displayed. A continuous wave seed source is injected into the parametric oscillator in the counter clockwise or backward direction for wavelength control. A pulsed pump is also injected into the parametric oscillator in the backward direction to bring the parametric oscillator to threshold. This

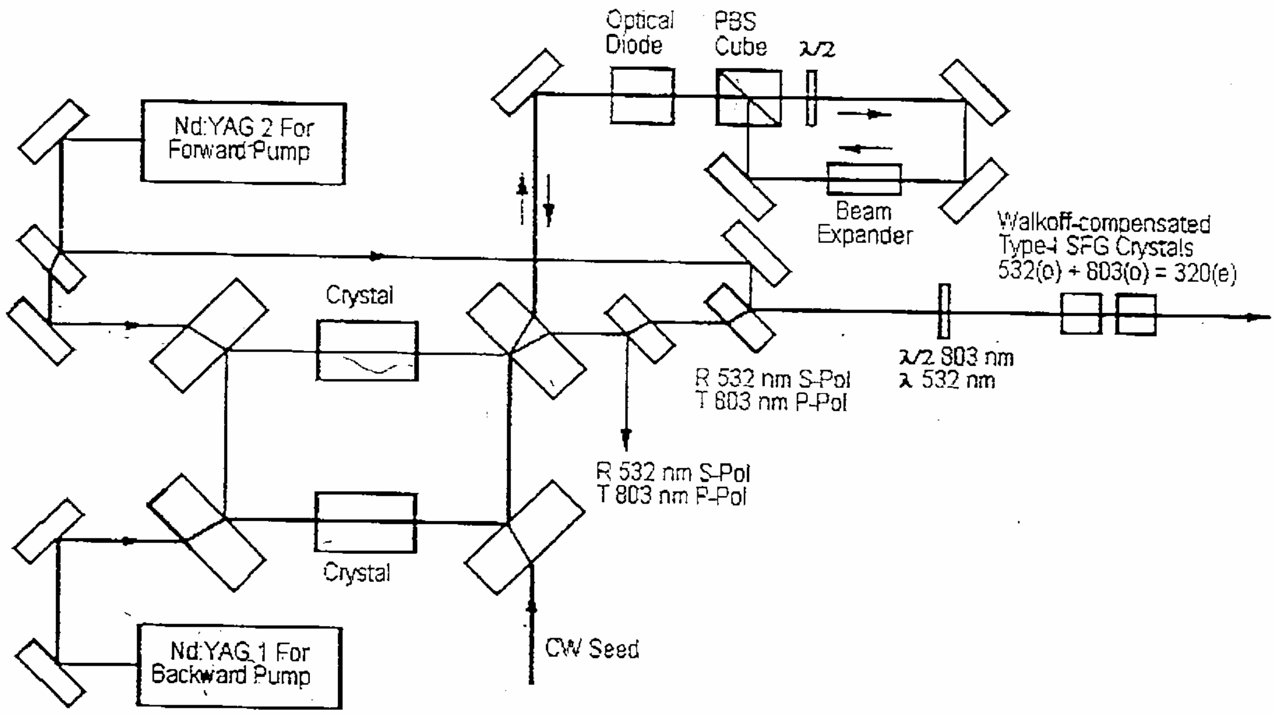

Figure 1. Simplified parametric oscillator
Courtesy Darrell Armstrong, Sandia

minimizes the pulse evolution time interval. When threshold is reached, the backward parametric oscillator in reversed and sent back into the parametric oscillator in the clockwise or forward direction. The seeded forward pulse can then extract energy from the pump over most of the main pump pulse. Employing this design, pump energy depletion reached 0.85. In the ideal case, 0.56 of the depleted pump energy appears as the signal pulse.

Solid state lasers when coupled with nonlinear optics can produce a line tunable ultraviolet source. An illustration of this is the frequency tripled and quadrupled Nd:YAG laser that produces an output at 0.355 and 0.266 μm. This approach has several advantages including the use of well developed Nd:YAG lasers, especially diode pumped Nd:YAG lasers, and nonlinear interactions that are simple to implement. However, questions concerning tunability need to be addressed.

Although the Nd:YAG 1.064 μm transition is well known, somewhat less well known [3] is that Nd:YAG operates efficiently on several other laser transitions as well. Work done at NASA Langley measured several important spectroscopic features such as the linewidth, $\Delta\nu$, and the emission cross section, σ_e, and the laser performance on the stronger of these transitions. Values for these parameters are listed in Table 2. Laser performance

is characterized by a threshold, E_{ETH}, and a slope efficiency, σ_s. Threshold and slope efficiency data were taken with a flash lamp pumped Nd:YAG laser operating in the TEM_{00} transverse mode. It may be noted that almost all of the slope efficiencies are more than 0.01. Slope efficiencies for multimode flash lamp pumped Nd:YAG lasers operating at 1.064 μm and in many transverse modes can reach on the order of 0.03. Thus, the efficiency penalty for operation on other transitions need not be severe.

To expand the possible ultraviolet wavelengths, the laser output at each of the transitions can be frequency tripled and quadrupled. This spans the spectral ranges from 0.440 to 0.452, 0.351 to 0.364, 0.330 to 0.339, and 0.263 to 0.281 μm. However, there is a large gap in the spectral range from 0.281 to 0.330 μm. This gap can be alleviated if a laser operating on a $^4F_{3/2}$ to $^4I_{11/2}$ transition could be mixed with a laser operating on a $^4F_{3/2}$ to $^4I_{13/2}$ transition. If so, wavelengths in the range from 0.293 to 0.307 could be generated. A standard method of approaching this would be to use 2 lasers and synchronize their pulses to within a small fraction of the pulse length, typically a few nanoseconds.

TABLE 2. Parameters of Nd:YAG $^4F_{3/2}$ to $^4I_{11/2}$ and $^4F_{3/2}$ to $^4I_{13/2}$ laser transitions

λ_L(μm)	$\sigma_e(10^{24}\ m^2)$	$\Delta\nu(cm^{-1})$	E_{ETH}(J)	σ_s
1.0520	9.62	5.7	4.93	0.0123
1.0614	20.62	4.8	2.60	0.0184
1.0641	27.74	6.0	1.99	0.0193
1.0737	15.15	5.2	3.62	0.0139
1.0779	6.26	9.9	7.63	0.0095
1.1120	3.97	12.1	10.28	0.0113
1.1160	3.95	14.4	11.48	0.0104
1.1225	3.97	11.4	11.26	0.0112

λ_L(μm)	$\sigma_e(10^{24}\ m^2)$	$\Delta\nu\ (cm^{-1})$	E_{ETH}(J)	σ_s
1.3187	8.92	4.5	6.64	0.0127
1.3336	4.03	3.7	11.82	0.0104
1.3381	9.57	5.0	6.53	0.0131
1.3564	7.35	6.6	8.42	0.0107

NASA Langley conceived and developed a single laser that generates synchronous Q-switched pulses from both the $^4F_{3/2}$ to $^4I_{11/2}$ transition and the $^4F_{3/2}$ to $^4I_{13/2}$ transition. Typically this does not occur because the transition with the highest round

trip gain will deplete the population inversion before pulses operating on other transitions can extract a significant amount of energy. However, by carefully designing the resonator, a single laser can produce synchronous and collinear pulses. In this case, sum or difference frequency generation becomes as simple as second harmonic generation. An optical schematic of the ultraviolet laser system appears in Figure 2. Because both pulses have the same output mirror and are produced in the same laser rod, they are collinear. Because both pulses have the same Q-switch, they are initiated at the same time. By careful resonator design, both pulses can have the same pulse evolution time interval. The inverse of the pulse evolution time interval when plotted versus pump energy can be shown to be a collinear straight lines for both the 1.052 and 1.319 μm transitions.

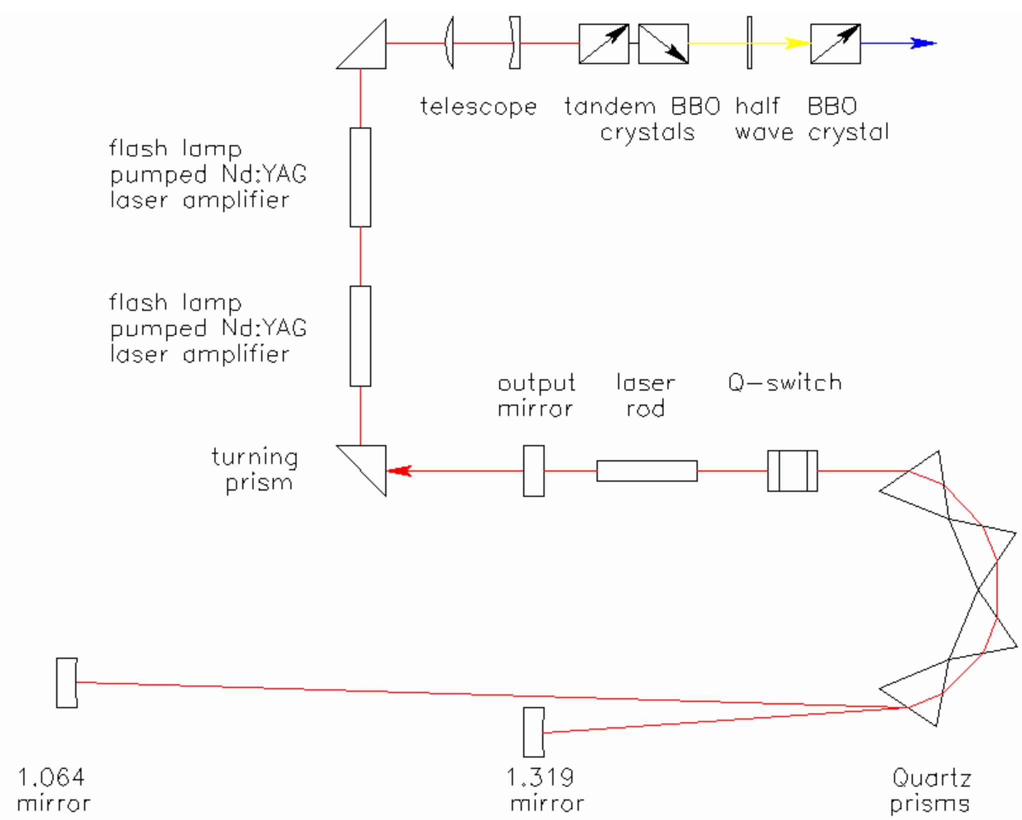

Figure 2. Optical schematic of STOP light laser

Given a single laser that synchronously generates both wavelengths for sum frequency generation, implementing this process becomes as simple as second harmonic generation. The Nd:YAG laser can designed to generate any pair of wavelengths from the $^4F_{3/2}$ to $^4I_{11/2}$ and the $^4F_{3/2}$ to $^4I_{13/2}$ transitions. With

the laser depicted in Figure 2, the tandem BBO crystals can be rotated through a small angle to produce second harmonic of 1.319 μm, the sum frequency of 1.319 and 1.052 μm, or the second harmonic of 1.052 μm. The resulting wavelengths are at 0.660 μm, red, 0.585 μm, orange, or 0.526 μm, green. The red, orange, and green laser pulses are reminiscent of a STOP light, giving rise to the acronym Synchronously Tunable Optical Pulses. Each of these sum frequency wavelengths can then be frequency doubled to the ultraviolet, in this case at 0.330, 0.293, or 0.263 μm.

A laser source for the remote sensing of water vapor can be based on diode pumped Nd lasers [4]. In this case, atmospheric scientists decided that 0.94411 μm was the best wavelength for this task. Methods of producing laser pulses at this wavelength include a parametric oscillator and a $Ti:Al_2O_3$ laser. However both methods require a frequency doubled Nd pump laser. A much simpler method would use a Nd laser to directly generate a laser output at 0.94411 μm. Nd:YAG has a transition in this region but the 0.946 μm wavelength is not right and the literature reported efficiency of flash lamp pumped laser was abysmally low.

3.0 Compositional tuning

NASA Langley developed the concept of compositional tuning to generate the correct wavelength. The chemical formula for YAG is actually $Y_3Al_5O_{12}$. If part of the Al is replaced by Ga, the wavelength of the transition tunes. By selecting the proper chemical composition, the $^4F_{3/2}$ to $^4I_{9/2}$ transition at 0.946 μm can be tuned to 0.9441 μm [4]. Spectroscopy at NASA Langley provided data for the wavelength of $Nd:Y_3Ga_xAl_{1-x}O_{12}$ as a function of the Ga concentration, given Figure 3. The wavelength of choice can be produced given the correct Ga concentration. Similar successful compositional tuning was demonstrated with $Nd:Y_3Sc_xAl_{1-x}O_{12}$.

Given that the laser can be compositionally tuned to the desired wavelength, the efficiency of a Nd laser operating on the $^4F_{3/2}$ to $^4I_{9/2}$ transition needed to be improved. A search of the literature indicated that the best performance of Nd:YAG when operating on the $^4F_{3/2}$ to $^4I_{9/2}$ transition was characterized by an operational temperature of 249 °K, a threshold of 62 J and a slope efficiency of 0.00012, as indicated in Table 3. A low operating temperature is helpful because this is a quasi 4 level laser. By improving the laser design, including shortening the laser rod and eliminating any unpumped regions of the laser rod, performance is vastly improved. The threshold was reduced by bonding undoped YAG onto the ends of the flash lamp pumped laser

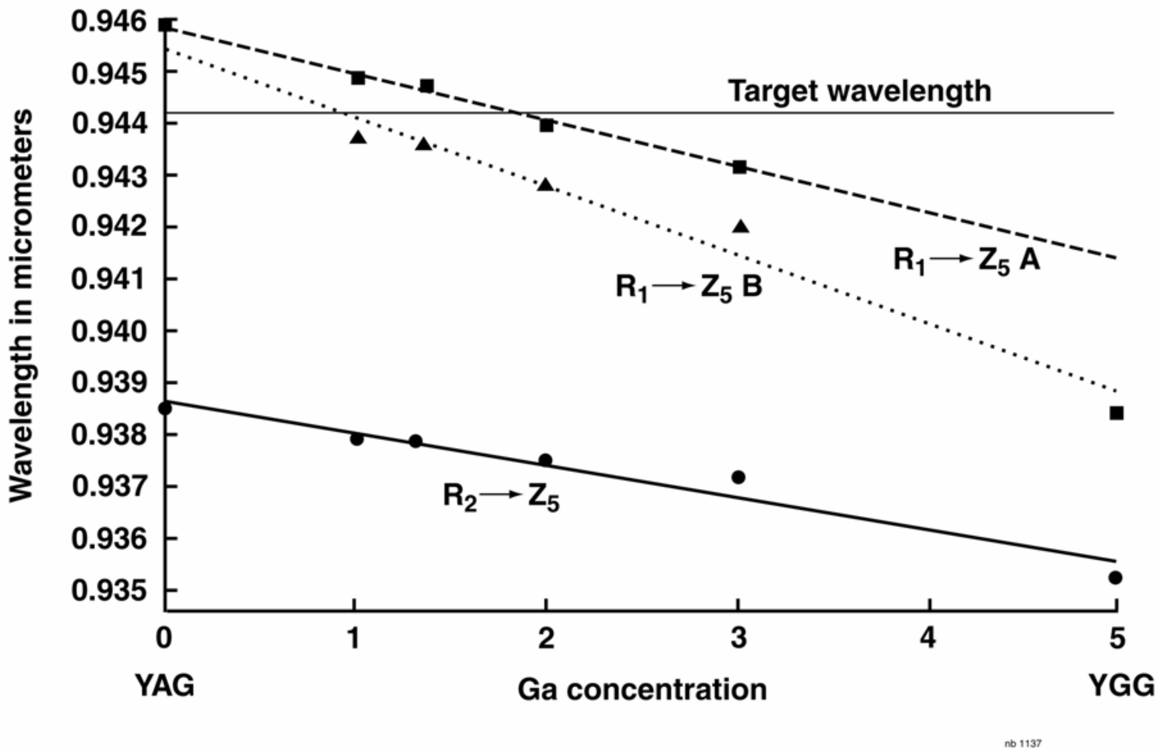

Figure 3. Compositional tuning of Nd:YGAG

rod, performance is vastly improved. The threshold was reduced by a factor of 5 while the slope efficiency was increased by a factor of 6. This was achieved in spite of the fact that the operating temperature was increased to nearly room temperature and the laser operated in TEM_{00} mode. It may be noted that the slope efficiency of a flash lamp pumped Nd:YAG operating multi transverse mode on the 1.064 μm transition can reach 0.03.

TABLE 3. Performance of Nd lasers on the $^4F_{3/2}$ to $^4I_{9/2}$ Transition

System	Nd:YAG literature	Nd:YAG LaRC	Nd:YAG LaRC	Nd:GYAG LaRC
Length	60 mm	48 mm	38 mm	50 mm
Ends	standard	standard	bonded	standard
Temp.	248°K	290°K	290°K	290°K
Threshold	62J	13.7J	11.7J	13.9J
Slope Eff.	0.0014	0.0067	0.0094	0.0096

Diode pumped Nd:YAG also demonstrated efficient Q-switched operation at 0.946 μm [6]. Multiple, end pumped, laser modules

were incorporated into a single oscillator. Resonator design confined operation to the TEM_{00} mode. An acousto optic modulator was employed as a Q-switch for the laser. With a single laser module in the resonator, an optical to optical, Q-switched slope efficiency of 0.147 was achieved. The laser pulse energy scales approximately linearly with the number of laser modules in the resonator. Employing 3 laser modules in the resonator, 75 mJ of energy was obtained in a TEM_{00} Q-switched pulse.

4.0 2.0 μm lasers and the mid infrared

Ho:Tm lasers, such as Ho:Tm:YLF or Ho:Tm:LuLF, have very complex dynamics because there are 2 different lanthanide series atoms in the laser material and there are many opportunities for energy transfer and energy sharing. Ho is a good candidate for a solid state laser because it has a both a long upper laser level lifetime and a reasonably large emission cross section. Unfortunately, it does not have strong absorption bands that correspond to commercially available laser diode arrays. Tm does have the strong absorption bands but its emission cross section is small making efficient energy extraction difficult. By combining both Ho and Tm in a single laser material obviates much of the difficulty. As shown in Figure 4, Tm absorbs the

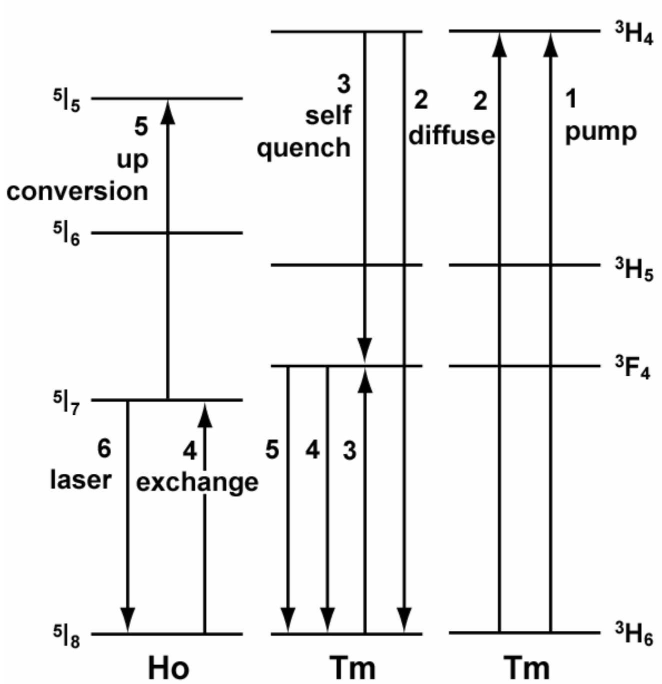

FIGURE 4. Simplified Ho:Tm laser dynamics

pump photon, process 1, ideally relaxes by self quenching to produce 2 Tm atoms in the $^3F_4$ manifold, process 3, and transfer the energy to the Ho $^5I_7$ manifold, process 4, from which the laser process occurs, process 6. There are also energy transfer processes such as diffusion, process 2, and the deleterious up conversion, process 5. Modeling of the Ho:Tm laser dynamics requires knowing about 30 parameters, many of which are quite difficult to measure.

A NASA Langley developed addition to a quantum mechanics model was used to calculate the requisite energy transfer and diffusion parameters. These parameters were then employed in a NASA Langley developed laser dynamics code to predict the gain of Ho:Tm:YLF lasers. Laser gain was also measured as a function of pump intensity using several Ho:Tm:YLF samples with different Ho and Tm concentrations. Typical results are shown in Figure 5 where both measured and predicted gain for both polarizations are shown for a Ho:Tm concentration of 0.015:0.040 [7]. Good agreement is apparent between the measured and predicted gain. Other Ho:Tm concentrations yielded similar supportive results. It should be noted that the predicted gain is not the result of curve fitting with adjustable parameters.

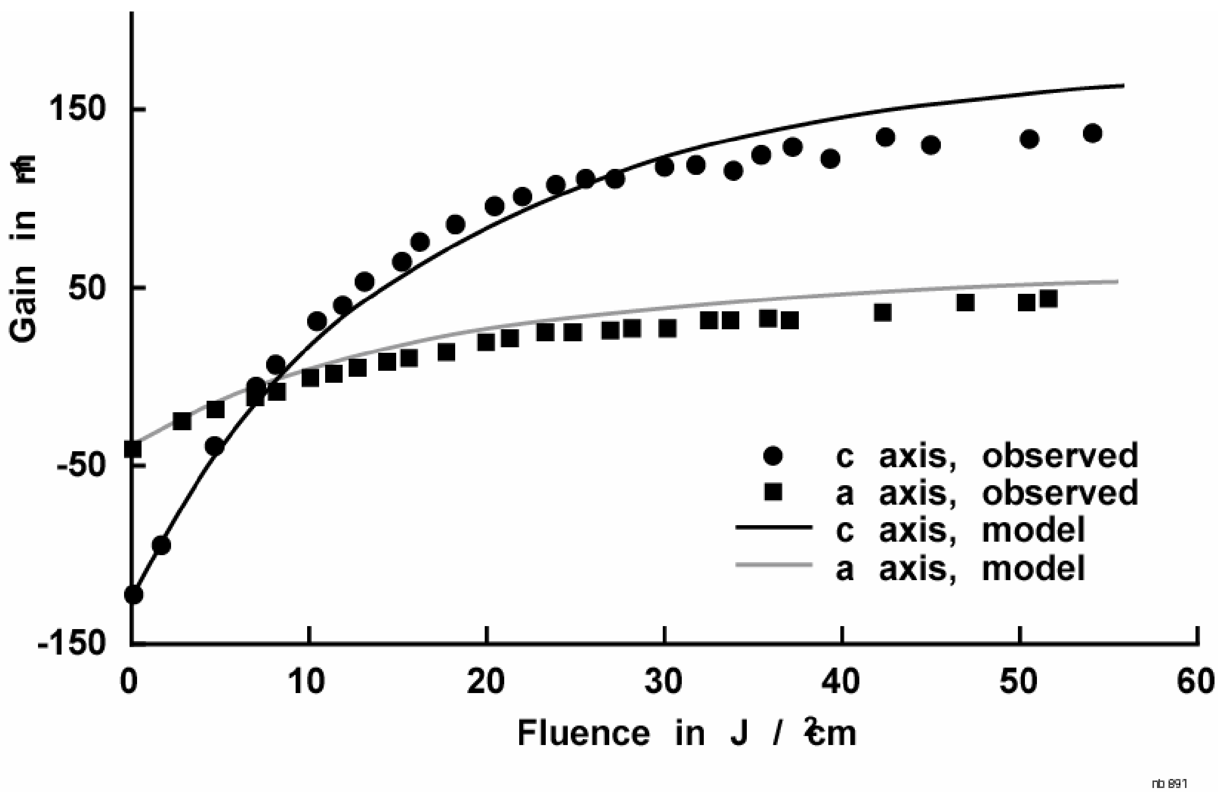

FIGURE 5. Measured and predicted gain in Ho:Tm:YLF

Quantum mechanical models were also employed to find 2.0 μm laser materials with performance superior to that of Ho:Tm:YLF. An empirical approach to finding a superior Ho:Tm laser material would be too costly and time consuming. Therefore, a quantum mechanical survey of isomorphs of YAG and YLF was undertaken to find a laser material superior to Ho:Tm:YAG or Ho:Tm:YLF. Based solely on these quantum mechanical calculations, Ho:Tm:LuAG was predicted to be superior to Ho:Tm:YAG. In addition, Ho:Tm:LuLF was predicted to be superior to Ho:Tm:YLF [8]. These laser materials were grown under contract and evaluated at Langley. Laser performance of Ho:Tm:LuLF and Ho:Tm:YLF are compared in Figure 6 [9]. It can be observed that Ho:Tm:LuLF performs significantly better than Ho:Tm:YLF. Total optical to optical efficiency of the former is over 0.13 even though the laser rod is operated at room temperature. The superiority of Ho:Tm:LuLF over Ho:Tm:YLF was verified by research in Japan. After these initial demonstrations, a room temperature Ho:Tm:LuLF oscillator and amplifier produced a 1.0 J/pulse Q-switched, in a single frequency, 1.1 diffraction limited output. The oscillator was completely conduction cooled by thermally bonding the laser rod to a heat sink that was cooled with using heat pipe technology.

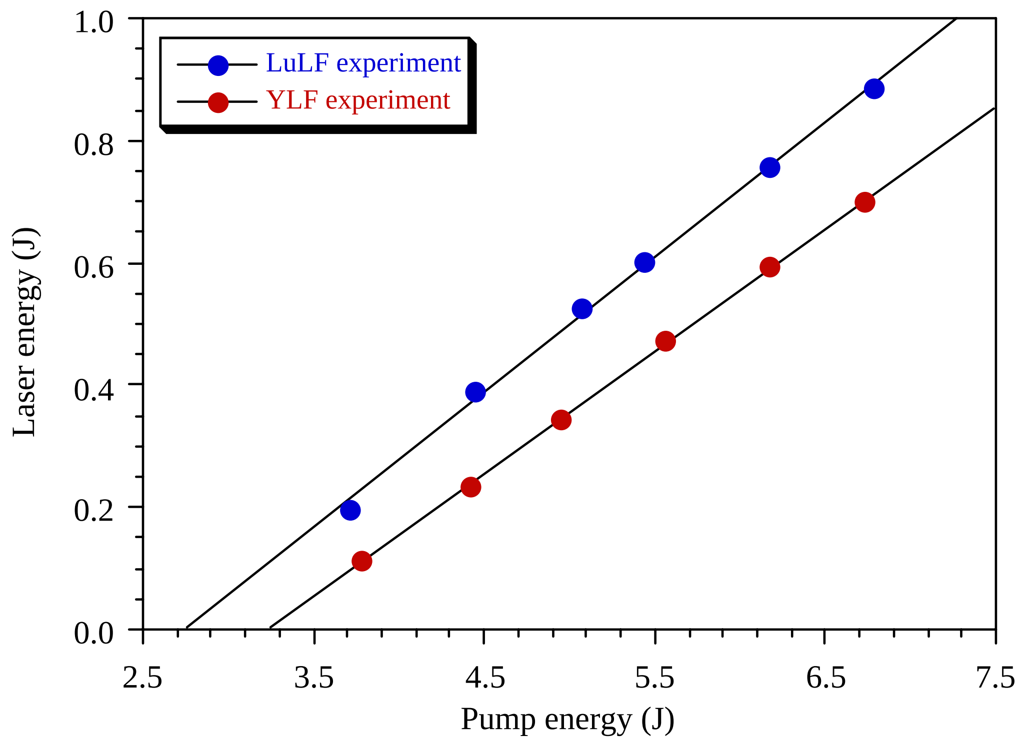

FIGURE 6. Performance of Ho:Tm:LuLF and Ho:Tm:YLF Courtesy of Jirong Yu, NASA Langley

Besides being an excellent laser source for coherent wind measurements, the Ho:Tm:LuLF laser can be used as a nominally eye safe source to measure H_2O and CO_2 or as a pump for a mid infrared parametric oscillator. NASA Langley demonstrated a $ZnGeP_2$ parametric oscillator pumped by a Q-switched 2.052 μm Ho:Tm:YLF laser. Output energy as high as 17.3 mJ at 4.8 μm was achieved. Threshold for this device was 6.0 mJ and the slope efficiency was slightly over 0.3. It may be noted that the ratio of photon energies limits the slope efficiency to 0.43. This device can be tuned from about 2.6 μm to 9.5 μm.

Injection seeding of a mid infrared parametric oscillator was initially demonstrated at NASA Langley [11]. Here a 1.73 μm Er:YLF laser pumped an $AgGaSe_2$ parametric oscillator. A 3.39 μm HeNe laser was used as the seed laser. Linewidth was measured by replacing the output slits of a 0.5 m monochromator with a pyroelectric vidicon. Because of the limited resolution of the pyroelectric vidicon, even the very narrow HeNe appeared to have a linewidth of ≈1.0 nm, shown in Figure 7. When unseeded, the parametric oscillator had a spectral bandwidth of 16 nm. When seeded, its spectral bandwidth was within the resolution limits.

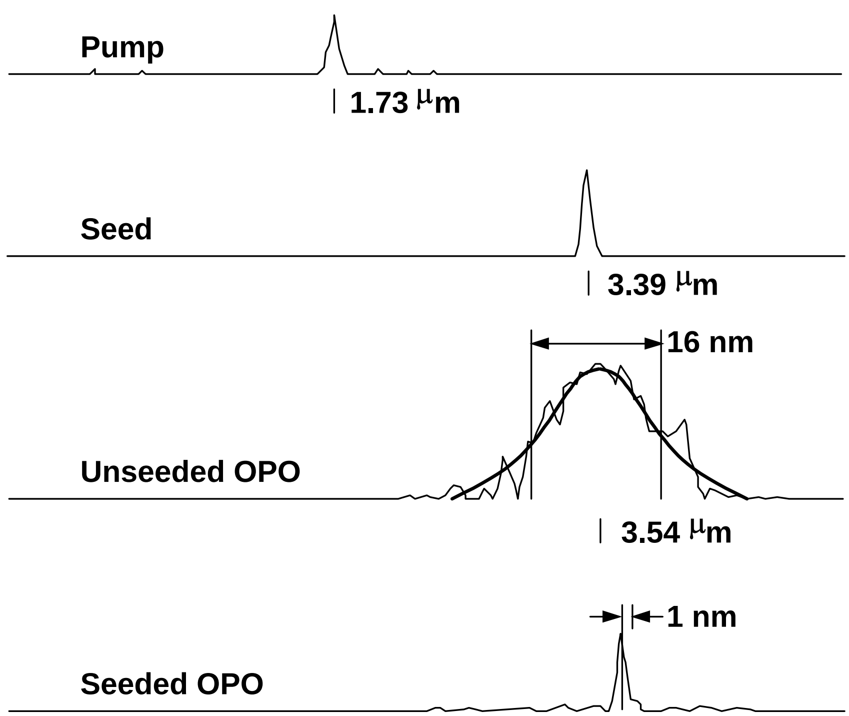

FIGURE 7. Seeded and unseeded $AgGaSe_2$ parametric oscillator spectral bandwidth

5.0 Summary

NASA develops efficient, high performance, solid state lasers primarily for remote sensing applications. These lasers are often unique devices that determine the state of the art. Development capabilities at NASA range from quantum mechanical and laser models to device construction for field applications. Specifically, 2 different approaches to a tunable ultraviolet laser were discussed. Although both approaches begin with a Nd:YAG laser, 1 device uses a parametric oscillator and the other uses a novel dual wavelength laser referred to as a STOP light laser. In the near infrared spectral region, a technique referred to as compositional tuning was used to invent a laser at a preselected wavelength. The wavelength was preselected by the atmospheric scientists to be best for the detection of H_2O. Great strides in 2.0 μm laser technology were made including: quantum mechanical and laser dynamics modeling, prediction of new and superior laser materials, and design and demonstration of field worthy devices. Finally, the 2.0 μm laser was used to pump a parametric oscillator capable of tuning over much of the mid infrared and injection seeding of the parametric oscillator was demonstrated.

1. F.E. Hovis, C. Culpepper, T. Schum, and G. Witt, "Single Frequency, 355 nm Source For Direct Detection Wind Lidar," Remote Sensing Of the Atmosphere, Ocean, Environment, And Space Conference, Honolulu, HI (2004)

2. D.J. Armstrong and A. Smith, "Optical Damage Resistant, 200 mJ, Nanosecond, Ultraviolet Light Source For Satellite Based Lidar Application, Material Research Society Spring Meeting, San Francisco, CA (2005)

3. N.P Barnes, B.M. Walsh, and R.E. Davis, "Dispersive Tuning And Performance Of A Pulsed Nd:YAG Laser," Advanced Solid State Photonics Conference, San Antonio TX, (2003)

4. B.M. Walsh, N.P. Barnes, D.J. Reichle, R.L. Hutcheson, and R.W. Equall, "Compositional Tuning Of Nd:YGAG To 0.94411 μm," Proceedings Of The Advanced Solid State Laser Conference, 416-418 (1998)

5. N.P Barnes, B.M. Walsh, R.L. Hutcheson, and R.W. Equall, “Pulsed $^4F_{3/2}$ to $^4I_{9/2}$ Operation Of Nd Lasers,” J. Opt. Soc. Am. B 16 2169-2177 (1999)

6. T.J. Axenson, N.P. Barnes, and D.J. Reichle, “High Energy Q-Switched 0.946 μm Diode Pumped Laser,” Proceedings Of The Advanced Solid State Laser Conference TOPS 50, 200-203 (2001)

7. N.P. Barnes, W.J. Rodriguez, and B.M. Walsh, "Ho:Tm:YLF Laser Amplifier Performance," J. Opt. Soc. Am. B, 13 2872-2882 (1996)

8. E.D. Filer, C.A. Morrison, and N.P. Barnes, "YLF Isomorphs For Ho And Tm Laser Applications," Advanced Solid State Laser Conference, Salt Lake City, UT (1994)

9. S. Chen, J. Yu, M. Petros, Y Bai, B.C. Trieu, M.J. Kavaya, and U.N. Singh, "One Joule, Double Pulsed Ho:Tm:LuLF Master Oscillator Power Amplifier (MOPA)," Advanced Solid State Photonics Conference Vienna, Austria, (2005)

10. H.R. Lee, J. Yu. N.P. Barnes, and Y. Bai, "High Pulse Energy $ZnGeP_2$ Singly Resonant OPO," Advanced Solid State Photonics Conference, Santa Fe, NM (2004)

11. N.P. Barnes, K.E. Murray, and G. Watson, "Injection Seeded Optical Parametric Oscillator," Proceedings On Advanced Solid State Laser Conference, 13, 356-360 (1992)